Article

Synthetic Strategies and Structural Aspects of Metal-Mediated Multiporphyrin Assemblies

Elisabetta Iengo, Ennio Zangrando, and Enzo Alessio

Acc. Chem. Res., **2006**, 39 (11), 841-851• DOI: 10.1021/ar040240+ • Publication Date (Web): 25 August 2006

Synthetic Strategies and Structural Aspects of Metal-Mediated Multiporphyrin Assemblies

ELISABETTA IENGO,†
ENNIO ZANGRANDO, AND ENZO ALESSIO*
Department of Chemistry, University of Trieste, 34127 Trieste, Italy

Received April 25, 2006

ABSTRACT
Porphyrins play a major role as active chromophores in artificial systems mimicking the natural photoinduced processes. The formation of coordination bonds between peripheral donor sites on the porphyrins and external metal fragments has proven to be an efficient alternative to covalent synthesis for the construction of multiporphyrin assemblies, whose complexity and beauty gradually approach those of the multichromophore systems found in nature. In a modular approach, relatively simple metal-mediated porphyrin adducts, owing to their thermodynamic and kinetic stability, can be exploited as building blocks in the construction of higher order architectures. Thus, multichromophore systems become accessible *on demand*, with a limited synthetic effort. The collection of solid-state structures reported here demonstrates that the flexibility of the porphyrins *and* the metal junctions, combined with the conformational freedom of the coordination bonds, may lead to assemblies with hardly predictable architectures. Examples in which X-ray structural determination was essential for establishing the real composition and geometry of the multiporphyrin assemblies are highlighted.

1. Introduction

Among many interesting light-induced functions, those inspired by natural photosynthesis have attracted special attention. As a result of extensive spectroscopic studies and detailed structural determinations, the *photoinduced charge separation* taking place in the reaction centers and the *antenna effect* carried out by the light-harvesting units are now understood in great detail.[1] Artificial systems mimicking the natural photoinduced processes are the subject of continuing research activity, fostered by the problem of solar energy conversion.[2] In many of these artificial systems, porphyrins (and/or metalloporphyrins) play a major role as active chromophores.[3] In fact, besides their chemical resemblance to the chlorophylls of the natural systems, porphyrins can be considered as ideal components for the construction of artificial systems because of several appealing features: rigid, planar geometries, high stability, inherent symmetry, and facile tunability of their optical and redox properties by metalation/functionalization.

Supramolecular synthetic strategies have emerged as efficient alternatives to covalent synthesis in the construction of large, robust, and shape-persistent multicomponent porphyrin architectures. Both coordination and multiple hydrogen bonds can be used as noncovalent binding forces, often in combination with other noncovalent and/or conventional covalent interactions.[4] Topologically controlled multiporphyrin arrays can be assembled by judicious design of the geometry of the building blocks.

Even though the ultimate aim of our work in this field concerns the photophysical properties and functions of metal-mediated assemblies of chromophores (that were reviewed recently),[5] in this Account, we will focus mainly on two topics, strictly related to their design: (i) the synthetic strategies that can be used for the construction of elaborated architectures and (ii) the X-ray structural features of the supramolecular assemblies (examples of metal-mediated assemblies lacking X-ray characterization will not be described here).

1.1. Synthetic Strategies. Many organic molecules employed as building blocks in hydrogen-bonded assemblies have a dual nature; i.e., they bear both donor and acceptor moieties for multiple bonding. This peculiar feature is seldom found in components for metal-driven assembling; most often, the electron-donor and -acceptor functionalities are on different fragments. Metalloporphyrins are an almost unique class of metal compounds that can behave both as Lewis donors and acceptors for the formation of new coordination bonds. In fact, provided that the inner metal is not coordinatively saturated and that the tetrapyrrole ring bears exocyclic coordinating groups, then metalloporphyrins can behave as ligands through the periphery and as Lewis acids through the metal core. The metal has normally one or two axial coordination sites available, while the binding sites at the porphyrin periphery range most commonly between one and four.

The assembling process, i.e., the formation of axial and/or peripheral coordination bonds, can occur with the metalloporphyrins themselves (self-coordination), with metalloporphyrins of a different nature, or with other donor and/or acceptor components. Dependent upon the

Elisabetta Iengo studied chemistry at the University of Trieste, where she received her "Laurea" in 1998 and Ph.D. in 2002. In the same year, she was awarded the prize for the best Ph.D. thesis in inorganic chemistry by the Italian Chemical Society. After 1 year of postdoctoral research in Strasbourg (France) and 3 years in Trieste, she is currently a Marie Curie Fellow at the University of Cambridge (U.K.).

Ennio Zangrando grew up in Trieste. He received his degree in chemistry from the University of Trieste in 1974, where he is now Associate Professor of inorganic chemistry. His research interest deal with X-ray crystallography, using conventional sources as well as synchrotron radiation. His work was dedicated to the structural properties of bioinorganic complexes and has been extended in recent years to supramolecular chemistry.

Enzo Alessio received his "Laurea" in chemistry from the University of Trieste in 1982 and his Ph.D. from the University of Ferrara (Italy) in 1989. In 1996, he was awarded the Nasini Prize to young researchers from the Italian Chemical Society. After a year of postdoctoral work at Emory University (Atlanta, GA), in 2000, he became Associate Professor of inorganic chemistry at the University of Trieste.

* To whom correspondence should be addressed. E-mail: alessi@univ.trieste.it.
† Current address: University of Cambridge, Chemical Laboratories, Lensfield Road, Cambridge CB2 1EW, U.K.

10.1021/ar040240+ CCC: $33.50
Published on Web 08/25/2006

Chart 1

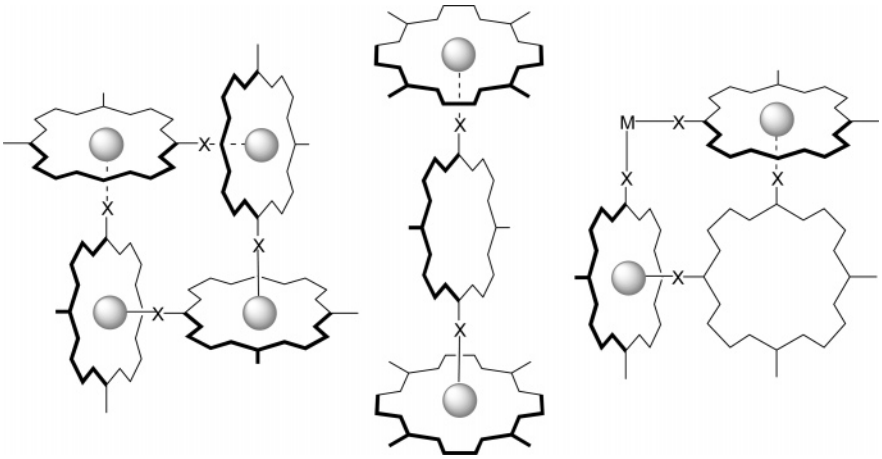

design of the building blocks, their ratio, and the concentration range employed, the process may lead preferentially to either discrete or polymeric assemblies or a mixture of both.[4] When the coordination bonds are inert, the mixing order of the building blocks becomes important and it can lead to the formation of kinetic compounds, different from the most thermodynamically stable one.

The donor/acceptor facet of metalloporphyrins can be elaborated by playing with the preference of the inner metal toward different electron donors (N, O, P, etc.).[6]

Finally, the reactive sites of the metalloporphyrin components do not necessarily become all saturated in the final product. Adducts with unreacted coordination sites can be isolated and eventually exploited for the construction of higher order assemblies in a hierarchical approach.

Viable acceptor units, other than the metalloporphyrins themselves, are coordination compounds with good leaving groups. To date, the most frequently used precursors for the efficient metal-mediated assembly of multiporphyrin adducts are complexes of Pd^{II} or Pt^{II}, Re^{I}, and Ru^{II}. Most of them share the common feature of bearing two *cis* positions easily available for coordination. The assembling process between the peripheral donor groups of the porphyrins and the external metal fragments occurs under thermodynamic control when relatively labile metal centers are used, while it is under kinetic control with inert metals (unless high temperatures are used). A judicious choice of the ancillary ligands at the coordination fragments allows us to fine-tune the charge and polarity (and thus solubility) of the final adduct and to introduce additional useful functionalities. Heterometallic adducts can be also prepared, usually through a stepwise synthetic approach.

Given these general premises (see Chart 1 for general examples), our synthetic strategy can be summarized as follows: (1) preparation of relatively simple adducts by ligation of porphyrins to coordination compounds, eventually followed by metalation of the porphyrins (i.e., introduction of new acceptor sites) and (2) exploitation of these adducts for the construction of higher order assemblies, either by self-coordination or by treatment with other polytopic ligand/metal fragments.

1.2. Structural Considerations. Over the years, we have collected a remarkable number of X-ray structures of metal-driven assemblies of porphyrins. Beside allowing us to gather a wealth of geometrical information on these systems, in particular with regard to their flexibility and deformability, the solid-state structures made us very cautious in assigning a complex supramolecular structure based only on solution data. Quite often, these systems are symmetrical, thus making nuclear magnetic resonance (NMR) spectroscopy insufficient to discriminate between a number of possible structures or conformations, and often, they are not amenable for mass spectrometry. Moreover, molecular modeling is not completely reliable with systems of increased dimension and complexity. X-ray structural analysis is, in some cases, the only way for establishing unambiguously the nature of a supramolecular architecture with the caveat that, when the binding interactions are relatively weak and labile, the species found in solution and in the crystals may be different (see section 4).

2. Metal Complexes with Coordinated Pyridylporphyrins

Meso-pyridyl/phenyl porphyrins (PyPs) or strictly related tetrapyrrolic chromophores[7] can provide geometrically well-defined connections to as many as four metal centers by coordination of the pyridyl groups. The peripheral N atom(s) of PyPs can be in either the 4′ or 3′ position. With 4′-PyPs, the exocyclic coordination bonds are established in the plane of the porphyrin, along the *meso* bond axes; with 3′-PyPs instead, because the *meso* pyridyl rings are tilted, the coordination bonds are directed out of the plane of the chromophore (Chart 2). The electronic properties and solubility of PyPs can be tuned by functionalization of the phenyl rings or the β-pyrrolic positions. For example, perfluorinated phenyl rings increase the electron-acceptor properties of the metalloporphyrins, while aliphatic chains increase solubility in organic solvents and bulky groups prevent stacking in solution.

Chart 2

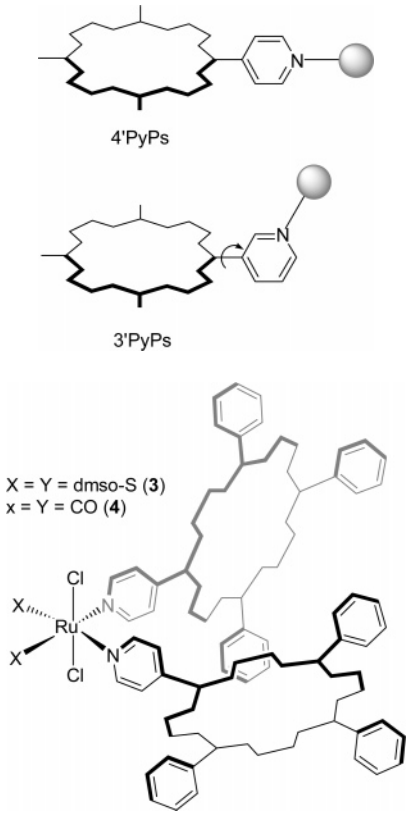

FIGURE 1. Schematic drawing of **3** and **4**.

The simplest metal-mediated multiporphyrin adducts are formed by two pyridylporphyrins bound to the same metal center. The metal precursor must therefore have two labile ligands, either *cis* or *trans* to each other. We mainly exploited two Ru^{II}−dmso complexes, *trans*-[$RuCl_2$(dmso-S)$_4$] (**1**) and *trans*,*cis*,*cis*-[$RuCl_2$(dmso-O)$_2$(CO)$_2$] (**2**), that behave as neutral *cis* bis-acceptor fragments upon selective replacement, under mild conditions, of two adjacent dmso ligands.[8,9] Thus, treatment of **1** or **2** with a slight excess of 4′-MPyP yielded the disubstituted complexes *trans*,*cis*,*cis*-[$RuCl_2$(dmso-S)$_2$(4′-MPyP)$_2$] (**3**) and *trans*,*cis*,*cis*-[$RuCl_2$(CO)$_2$(4′-MPyP)$_2$] (**4**), respectively (Figure 1).[10] The corresponding 3′-MPyP derivatives were similarly obtained. Recently, we also prepared the *cis* disubstituted ruthenium−nitrosyl complex *mer*-[$RuCl_3$(NO)(4′-MPyP)$_2$] (**5**) by treatment of the anionic precursor [*n*Bu_4N]*trans*-[$RuCl_4$(NO)(dmso-O)] with excess 4′-MPyP.[11] A square planar analogue of the bisporphyrin complexes **3**−**5**, *cis*-[Pd(dppp)(4′-*p*-tolylMPyP)$_2$](OTf)$_2$ [**6**, dppp = bis(diphenylphosphino)propane], was described by Woo and co-workers.[12]

The solid-state structures of **5** and **6** show significant differences in the geometries of the *cis* bis-pyridyl fragments (Figure 2). In the neutral ruthenium complex **5**, the distance between the porphyrin centroids is 14.9 Å. The angle defined by the metal center and the two porphyrin centroids is 98.7°, and that between the porphyrin mean planes is 83.78°. The corresponding parameters for the charged diphosphine palladium complex **6** are 9.1 Å and 56.1° and 20.4°, respectively, indicating that the two porphyrin ligands are strongly distorted (the Pd atom is sandwiched between the triflate counteranions, with Pd···O distances of 2.79 and 4.03 Å). The tilt angles of the coordinated pyridyl rings in **6** also indicate distortion from ideal geometry [Pd−N(py)−C_{para} = 157°, instead of 180°]. Rather than the different coordination geometries of the two metal ions, these marked differences might be ascribed to the nature of the ancillary ligands that are modestly hindering in the *mer*-$RuCl_3$(NO) fragment and quite sterically demanding in *cis*-$Pd(dppp)^{2+}$. Specific stacking interactions between the phenyl rings of the dppp bridge and the porphyrin pyridyl groups (Figure 2) may also play a role (see also section 3). However, packing forces are not to be excluded in defining the geometrical arrangement of the porphyrins.

NMR evidence shows that, in solution, the two adjacent porphyrins in **3**−**5** are in free rotation about the N(py)−Ru bonds. Zinc insertion thus provides two acceptor axial sites at a distance of 10.0−14.0 Å. Once in the porphyrin core, zinc likes to be five-coordinate and has a preference for N donors. Thus, **3**−**5** can behave as tweezers for appropriate ditopic nitrogen ligands when their two neighboring porphyrins are facing each other. The existing Ru−pyridyl bonds are stable and inert; therefore, no decomposition or scrambling processes occur upon treatment with N ligands. In particular, the zinc porphyrins in **3**−**5** have geometrical parameters that match perfectly the coordination of a 4′-*cis*-dipyridylporphyrin (Chart 1). Work toward the structural characterization of such tris-porphyrin macrocycles, in which 4-*cis*-DPyP is orthogonal to the other two, is in progress in our laboratory.

Compounds **3**−**5** can be thought of as the inorganic analogues of the porphyrin tweezer **7**, developed by Sauvage and co-workers, that features two oblique zinc(tris-*t*butylphenyl)porphyrins connected through a phenanthroline moiety. Compound **7** was proven to be an excellent host for 4′-*cis*-DPyP.[13] The molecular structure of [4′-*cis*-DPyP⊂**7**] shows the almost perfect geometrical match between the two interacting units (Figure 3). The excellent complementarity of the two components is confirmed by the Zn···Zn distance of 14.04 Å, only slightly longer than that found in **7** alone.[14] The phenanthroline and 4′-*cis*-DPyP moieties, nearly coplanar, are oriented normally to the zinc−porphyrins, which form a dihedral angle of 66.2°.

Compounds **3**−**5** present at least two advantages over **7** and other organic tweezer systems: (i) their synthesis is simpler, and (ii) the metal center and its ancillary ligands (and therefore the charge and solubility of the complex) can be varied "on demand".

To our knowledge, there is only one well-characterized example of a bis-pyridylporphyrin metal complex with *trans* geometry,[15] namely, the neutral palladium complex *trans*-[$PdCl_2$(3′-MPyP)$_2$] (**8**) obtained by Reed, Boyd, and co-workers by the reaction of *trans*-$PdCl_2$(dmso)$_2$ with 3,5-di-*t*butylphenyl substituted 3′-MPyP.[16] Owing to the kinked orientation of the porphyrin core with respect to the 3′-N(py)−Pd bond, the two porphyrins in **8** can assume an

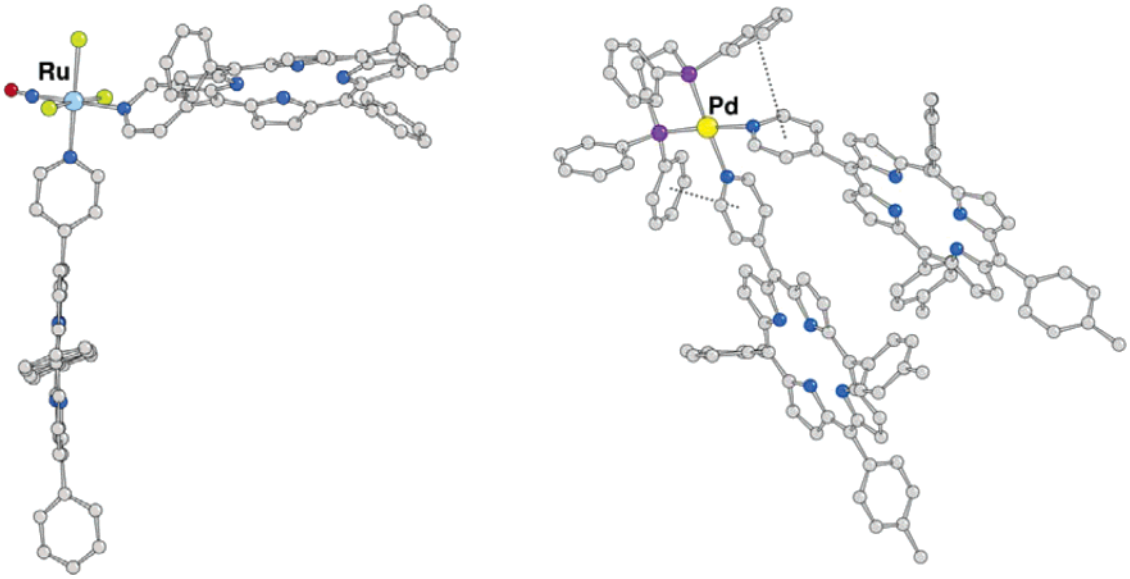

FIGURE 2. Perspective views of the X-ray molecular structures of **5** (left) and the cation of **6** (right). Stacking interactions in **6** are evident. Adapted from refs 11 and 12, respectively.

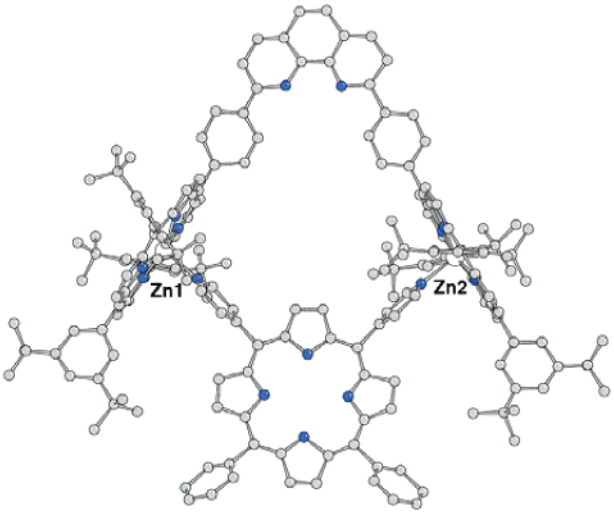

FIGURE 3. X-ray molecular structure (top view) of the tris-porphyrin macrocyclic assembly [4′-*cis*-DPyP⊂**7**]. Adapted from ref 13.

almost face-to-face orientation despite having a *trans* coordination geometry. Indeed, **8** was proven to be an efficient host for fullerene-type molecules through the jaw-like cleft defined by the two porphyrins. Figure 4 shows the molecular structure of the *trans*-[$PdCl_2$(Pd•3′-MPyP)$_2$]/C_{60} cocrystallate; C_{60} is symmetrically centered over the porphyrin rings, with the closest Pd···C distance being ca. 2.856 Å. Similar X-ray structures of jaws porphyrins/C_{60} and C_{70} cocrystallates were later reported by the same authors (porphyrin−porphyrin centroid distances of 11.5−12.0 Å and interplanar porphyrin angles of 40−60°).

This example demonstrates the greater conformational freedom of 3′-PyPs compared to 4′-PyPs and their superior potentialities in supramolecular design. In general, however, the final geometries of assemblies incorporating kinked porphyrins are hardly predictable *a priori* (see section 5).

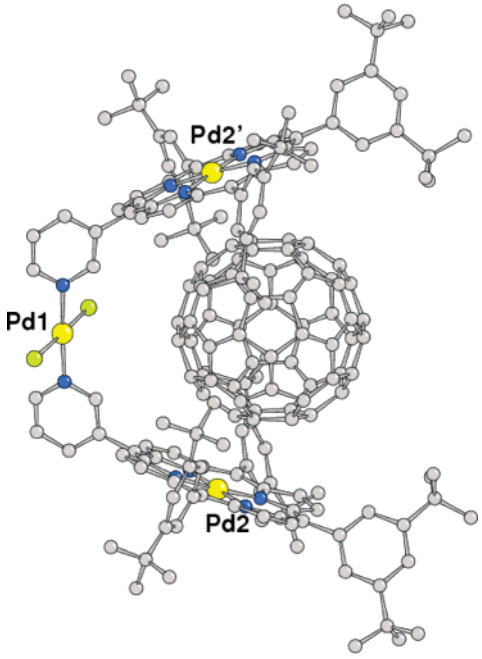

FIGURE 4. X-ray molecular structure of the **8**/C_{60} cocrystallate (porphyrins only partially occupied by Pd2). Adapted from ref 16a.

3. Metallacycles and Self-Coordination Products

When precursors **1** or **2** were treated with an excess of 4′-*cis*-DPyP, compounds *trans*,*cis*,*cis*-[$RuCl_2$(dmso-S)$_2$(4′-*cis*-DPyP)$_2$] (**9**) or *trans*,*cis*,*cis*-[$RuCl_2(CO)_2$(4′-*cis*-DPyP)$_2$] (**10**) were isolated.[17] These two bisporphyrin adducts are geometrical analogues of **3** and **4**, respectively, but feature two residual donor sites at their periphery [the 4′-N(py) groups] available for further coordination and thus are examples of *metal complex ligands*. We exploited the coordinating capability of **9** and **10** in two different ways (Scheme 1).

Scheme 1

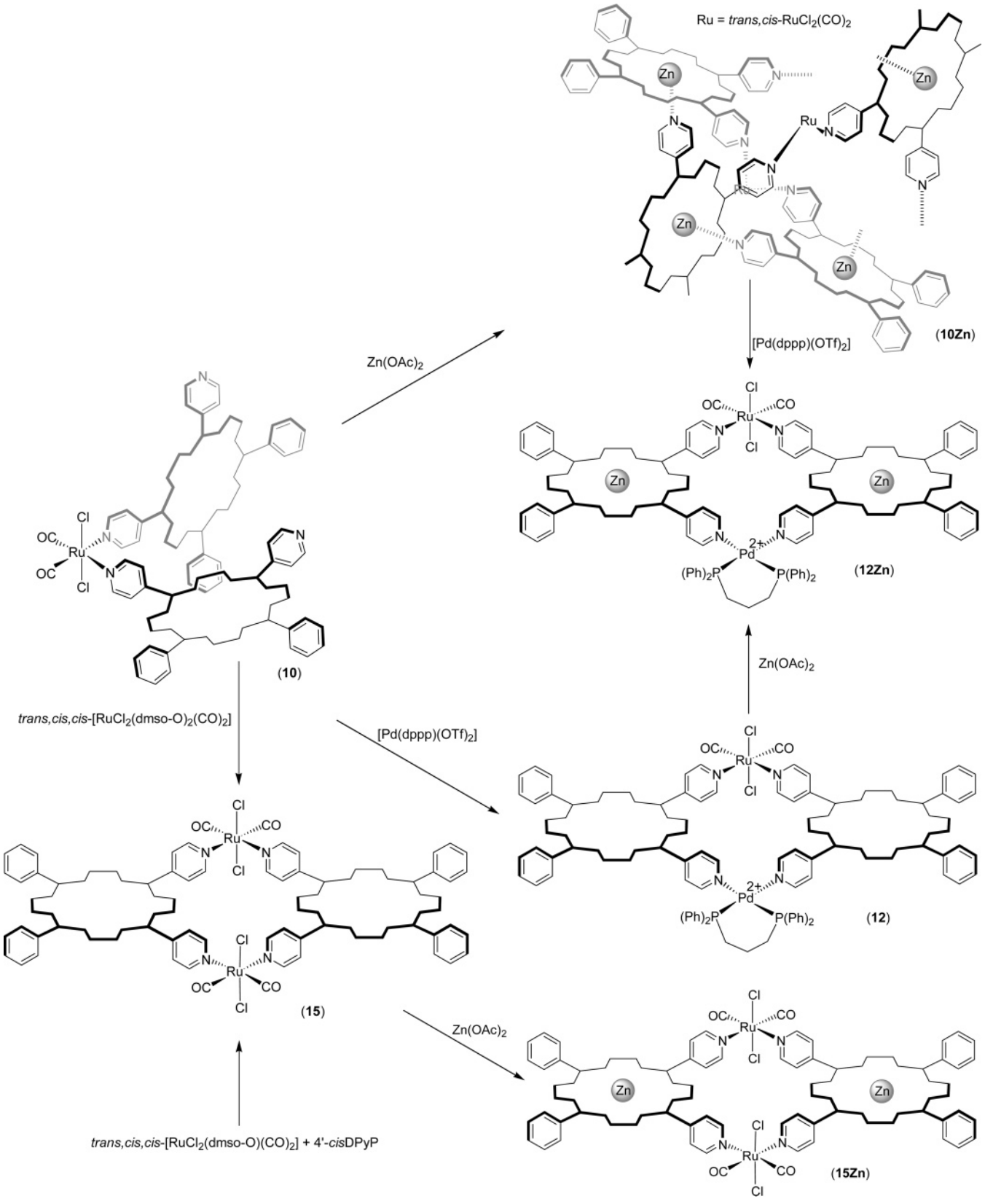

3.1. Two-Point Self-Coordination. Insertion of Zn^{II} into the two porphyrins of **10** yielded *trans,cis,cis*-[$RuCl_2(CO)_2$-(Zn•4′-*cis*-DPyP)$_2$] (**10Zn**), which is a novel type of metal-containing building block featuring two *donor* [the uncoordinated 4′-N(py) atoms] and two *acceptor* sites (the Zn atoms), capable of self-coordination.[18] Owing to the rotational freedom of zincporphyrins in **10Zn**, it is difficult to predict the outcome of the self-coordination process that could lead to discrete and/or polymeric species. ^{1}H NMR spectroscopy and single-crystal X-ray analysis es-

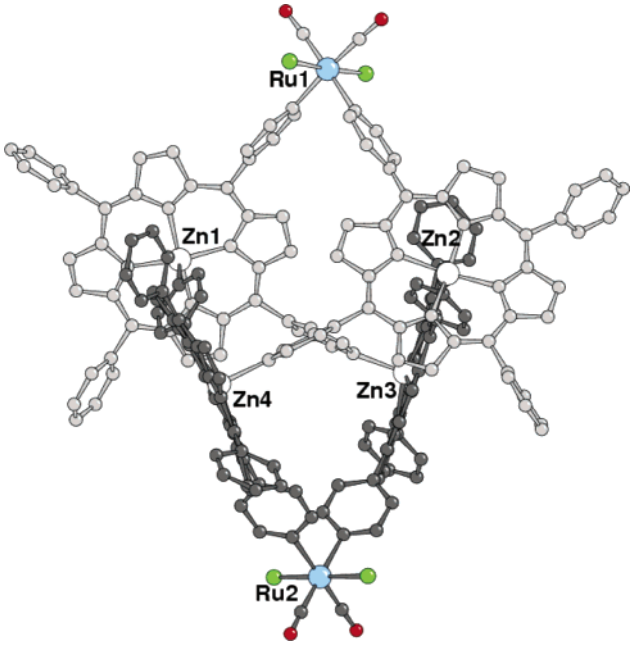

FIGURE 5. Molecular structure of [**10Zn**]$_2$, with *trans,cis,cis*-[$RuCl_2(CO)_2$(Zn·4′-*cis*-DPyP)$_2$] fragments in different shades. Adapted from ref 19.

tablished that **10Zn** self-assembles selectively to give the stable dimeric species [**10Zn**]$_2$, a *meso* pseudo-helicate, in which the two 4′-N(py) and the two zinc sites of one **10Zn** unit axially coordinate the complementary sites of the second unit (Figure 5).[19] The four Zn ions in [**10Zn**]$_2$ occupy the vertices of an irregular tetrahedron. The Zn···Zn distance in each **10Zn** unit is ca. 12.46 Å, while that between two different **10Zn** units is shorter and averages 9.83 Å. The Ru ions are 19.6 Å apart. To achieve the two-point self-coordination, the porphyrin planes of each **10Zn** unit form a dihedral angle in the narrow range of 42−45°. An estimation of the molecular size of [**10Zn**]$_2$ is provided by the distances between the carbonyl oxygen atoms of the two Ru ions, of about 24.0 Å. The small internal cavity hosts two chloroform molecules.

The adduct [**10Zn**]$_2$, which features four porphyrins and six metal atoms, is an unprecedented example of a discrete and highly ordered array of porphyrins obtained by two-point metal-mediated self-coordination. In the future, we aim to make new multipoint ruthenium−porphyrin building blocks by increasing the number of donor/acceptor pairs and by changing the geometrical parameters (e.g., 3′-PyPs instead of 4′-PyPs and *trans*-DPyP instead of *cis*-DPyP).

3.2. Metallacycles of Porphyrins. The hetero-bimetallic 2 + 2 metallacycles of porphyrins [Pd(dppp){$RuCl_2(X)_2$}-(μ-4′-*cis*-DPyP)$_2$](CF_3SO_3)$_2$ (X = dmso-S, **11**; X = CO, **12**), featuring one neutral octahedral Ru^{II} and one dicationic square-planar Pd^{II} fragment at opposite corners, were quantitatively assembled by titration of the *cis* bis-acceptor metal fragment [Pd(dppp)(CF_3SO_3)$_2$] into chloroform solutions of either **9** or **10** (Scheme 1).[17] The X-ray structure of **12** is shown in Figure 6. The metal−porphyrin center distances are about 9.83 Å, and the diagonal Pd···Ru distance is ca. 14.0 Å. The corresponding palladium metallacycle [Pd(dppp)(μ-4′-*cis*-DPyP)$_2$](CF_3SO_3)$_4$ (**13**), described by Stang and co-workers, has a similar rhomboid-type structure with a Pd···Pd distance of 14.1 Å (Figure 6).[20] Interestingly, in the solid state, these metallacycles adopt butterfly geometries, with dihedral angles between the two porphyrins of 138° and 133°, respectively. Such orientations are very likely due to stacking interactions between a phenyl ring of dppp and the pyridyl rings of the porphyrins (stacking distance in **12** of ca. 3.1 Å). In both complexes, the triflate counteranions are located in sets of two above and below the coordination plane of each Pd atom (Pd···O distances of 3.86 and 2.93 Å in **12** and in the range of 2.99−3.86 Å in **13**).

When [Pd(dppp)(OTf)$_2$] was titrated into a $CHCl_3$ solution of [**10Zn**]$_2$, the heterotrimetallic metallacycle of porphyrins [Pd(dppp){$RuCl_2(CO)_2$}(μ-Zn·4′-*cis*-DPyP)$_2$]-(CF_3SO_3)$_2$ (**12Zn**) was quantitatively obtained. Alternatively, **12Zn** was formed by the treatment of **12** with a slight excess of zinc acetate (Scheme 1).

Finally, the treatment of **9** with **1** or **10** with **2** led to the formation of the homometallic neutral metallacycles of porphyrins [$RuCl_2$(dmso-S)$_2$(μ-4′-*cis*-DPyP)]$_2$ (**14**) or [$RuCl_2(CO)_2$(μ-4′-*cis*-DPyP)]$_2$ (**15**). The same assemblies were obtained in one-pot reactions by the treatment of **1** or **2** with equimolar amounts of 4′-*cis*-DPyP. Metalation of **15** with zinc acetate led to the isolation of [$RuCl_2(CO)_2$-(Zn·4′-*cis*-DPyP)]$_2$ (**15Zn**) in pure form.[21] The X-ray structure shows that **15Zn** is almost perfectly flat, with a Ru···Ru distance of 14.01 Å (Figure 7).[22]

In comparison to the neutral 2 + 2 metallacycles of porphyrins reported by Hupp and co-workers,[23] which feature octahedral *fac*-[ReX$(CO)_3$] corner units (X = Br or Cl), **14** and **15** have the advantage of being more symmetrical; the two axial ligands of the Re^{I} corners are different (one halide and one CO), thus generating mixtures of isomers when more units are present in the same assembly. In addition, reactions leading to metallacycles are performed at room temperature with **1** and **2**, whereas prolonged heating is required for the [$ReX(CO)_5$] precursors. On the other hand, while the rhenium−porphyrin assemblies are thermodynamic products and thus obtained with high yields and purities, the ruthenium cyclic assemblies are kinetic products, formed in lower yields and often needing column purification. Nevertheless, under kinetic conditions, products with different stoichiometry, such as the reactive bisporphyrin complexes **9** and **10**, become accessible.

4. Higher Order Assemblies

As noted above for the bisporphyrin complexes **3**−**5**, owing to the thermodynamic and kinetic stability of the Ru−pyridyl bonds, solutions of **15Zn** can bind two further axial N ligands while remaining intact. Thus, **15Zn** is a 2D module with two axial junctions that can be exploited for the construction of more elaborate supramolecular adducts upon treatment with appropriate polytopic ligands.

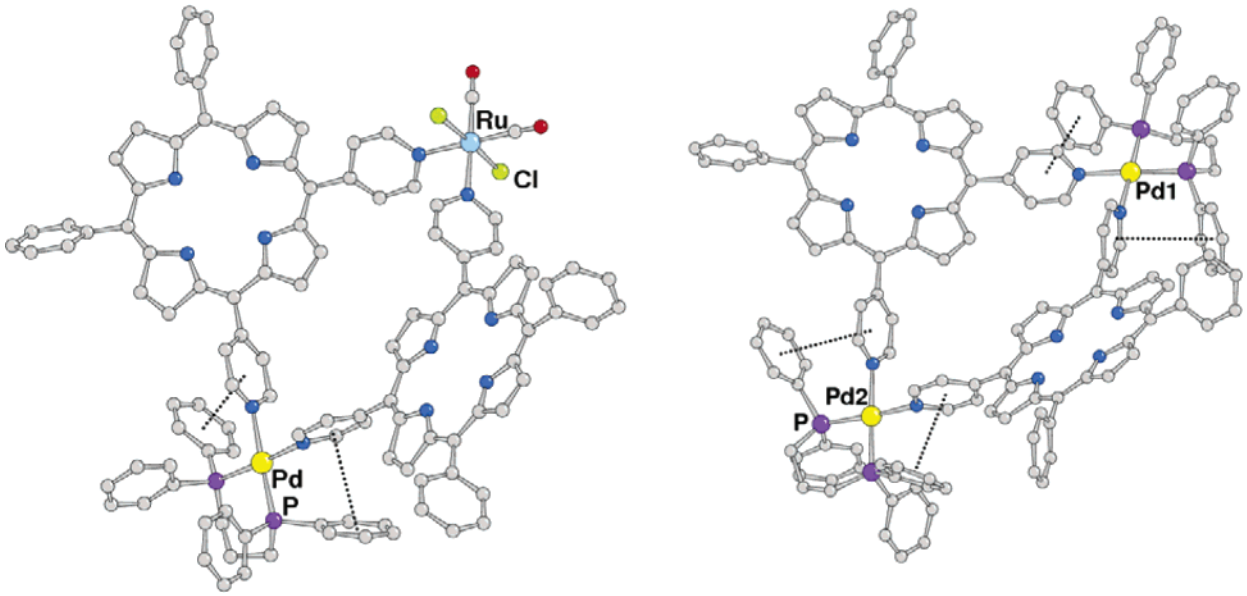

FIGURE 6. X-ray molecular structures of the cations of **12** (left) and **13** (right). Stacking interactions between the dppp ligand and the pyridyl rings are evident. Adapted from refs 17 and 20, respectively.

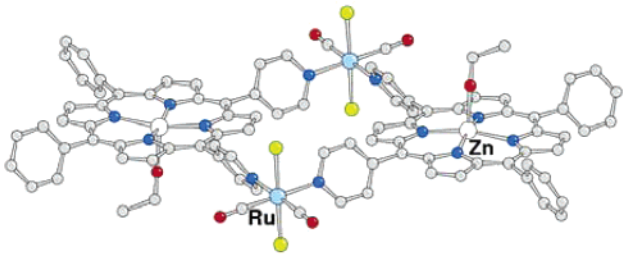

FIGURE 7. X-ray molecular structure of **15Zn**, adapted from ref 22. Two ethanol molecules are axially bonded to the Zn ions.

The relatively rigid frame of the porphyrin metallacycles ensures that the bridging ligands are arranged at a fixed distance.

Thus, as unambiguously evident by NMR spectroscopy, titration of $CDCl_3$ solutions of **15Zn** with one equivalent of a linear ditopic N ligand leads rapidly to the quantitative assembling of sandwich-like 2:2 supramolecular adducts of formula $[(\mathbf{15Zn})_2(\mu\text{-L})_2]$ (L = 4,4′-bipy, **16**; L = 4′-*trans*-DPyP, **17**; L = 4′-*trans*-DPyP-npm, **18**; estimated formation constants higher than 10^{18} M^{-3}), composed of two parallel metallacycles connected by two bridging ligands, which are axially bound to the zinc−porphyrins (Scheme 2).[21] Compounds **17** and **18**, that feature six porphyrins each, might be rightly defined as multiporphyrin molecular boxes. The solid-state X-ray structure of **17** shows that the distance between the two opposite metallacycles is ca. 19.5 Å and that the apical Zn−4′-N(py) bonds are approximately perpendicular to the porphyrin planes (Figure 8). The two bridging 4′-*trans*-DPyP ligands are cofacial and slightly bowed inward, at a distance of ca. 11.4 Å. The diagonal Ru···Ru and Zn···Zn distances for each metallacycle (slightly bent outward) are both very close to 14.0 Å, as in **15Zn** (see above).

The $CDCl_3$ ^1H NMR spectrum of **17** is perfectly consistent with the solid-state structure, suggesting that the same geometry, including the cofacial orientation of the two bridging pyridylporphyrins, is maintained in solution. Systems in which two cofacial porphyrins are connected to one another by organic bridges are well-known, but metal-mediated analogues are rather uncommon. Hupp and co-workers described large rectangle-shaped systems that feature two cofacial ethynylpyridyl zinc−porphyrins (the long edges, 24.5 Å), held in that position by coordination to either $[fac\text{-}\{Re(CO)_3\}_2(\mu\text{-2,2′-bipyrimidine})]^{2+}$ (**19**, Figure 9) or $[fac\text{-}\{Re(CO)_3]\}_2(\mu\text{-bisbenzimidazolate})]$ (**20**) fragments (the short edges). Interestingly, while the Re···Re distance along the short edge of the rectangle is 5.7 Å, the porphyrin walls approach within van der Waals distances (ca. 3.4 Å) because of strong stacking interactions.[24]

The solid-state architecture of the 4,4′-bipy derivative **16**, characterized by X-ray diffraction analysis, was found different from that detected in solution. It consists of an unprecedented infinite wire of **15Zn** metallacycles bridged on the two opposite faces by axially coordinated 4,4′-bipy connectors (Figure 10).[21]

The different structures found for **16** in solution (discrete) and in the solid state (polymeric) require the presence of an equilibrium between the two forms; very likely solubility reasons drive the equilibrium toward the polymeric arrangement upon crystallization. In solution, in all of the concentration ranges investigated, there is no spectroscopic evidence of an equilibrium between the discrete sandwich structure of **16** and polymeric material in detectable amounts.

5. Slipped-Cofacial Porphyrin Metallacycles

Treatment of precursor **2** with an equimolar amount of 3′-*cis*-DPyP rather than 4′-*cis*-DPyP yielded the corresponding neutral metallacycle $[RuCl_2(CO)_2(\mu\text{-3-}cis\text{-DPyP})]_2$ (**21**). X-ray structural investigation showed that in the solid state **21** has an unprecedented staggered geometry with

Scheme 2

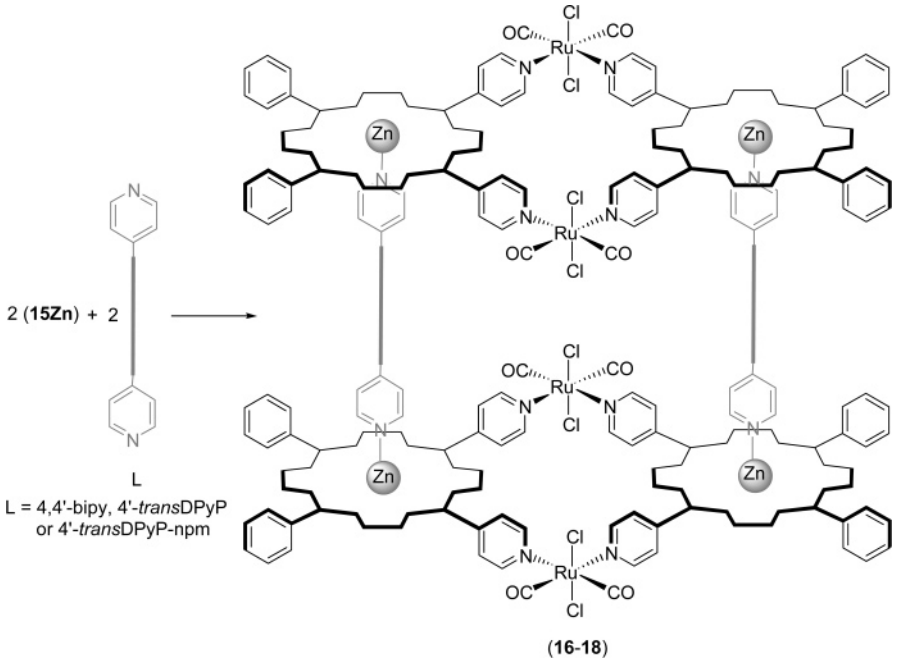

the two chromophores held in a *slipped-cofacial* arrangement by the external Ru^{II} metal fragments (Figure 11).[22] Both 3′-pyridyl rings on each porphyrin have a *syn* orientation with respect to the mean plane of the chromophore (dihedral angles of 45.5° and 61.7°), and the two Ru atoms are located above one porphyrin and below the other (*up*−*down* conformer).

The geometry of the two chromophores in **21** is reminiscent of those found for the two bacteriophylls of the special pair and for adjacent B850 units in the antenna systems of photosynthetic bacteria.[1]

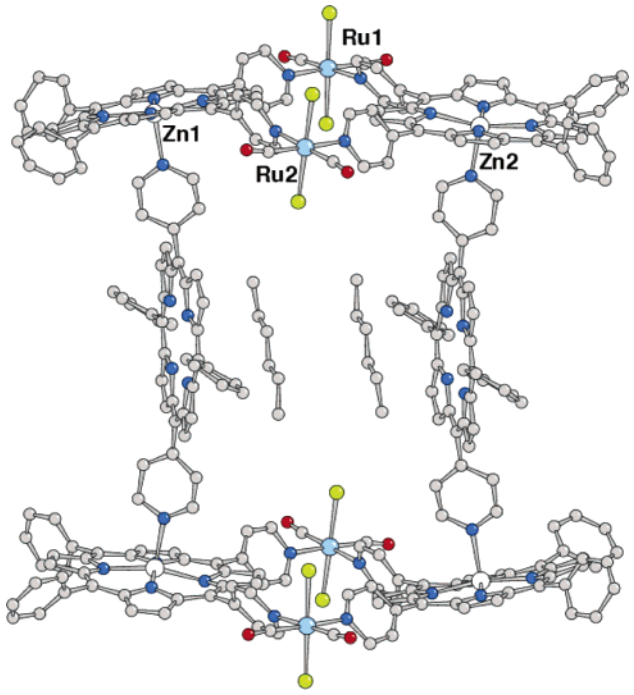

FIGURE 8. X-ray molecular structure of the molecular box of porphyrins **17**. Two molecules of *n*-hexane from crystallization are encapsulated in the cavity. Adapted from ref 21.

NMR spectroscopy is fully consistent with the solid-state structure of **21**, which is thus maintained also in solution. We had no evidence of the formation of other possible conformers of **21**, which might derive from different orientations of the 3′-N(py) rings. Models show that another highly symmetrical limiting geometry for **21** is that in which both 3′-pyridyl rings on each porphyrin maintain a *syn* orientation but the two Ru atoms are above both porphyrins, which are thus facing each other with a narrow dihedral angle (*up*−*up* conformer). The experimental ^{1}H NMR spectrum is not consistent with this conformer, and an equilibrium between different conformations was not detected by VT NMR experiments.[22] The fully zincated derivative $[RuCl_2(CO)_2(\mu\text{-Zn·3′-}cis\text{-DPyP})]_2$ (**21Zn**) was also structurally characterized and showed a geometry closely comparable to that of **21**. Similar dmso and mixed dmso/CO staggered metallacycles, $[RuCl_2(\text{dmso-S})_2(\mu\text{-3′-}cis\text{-DPyP})]_2$ (**22**) and $[RuCl_2(CO)(\text{dmso-S})(\mu\text{-3′-}cis\text{-DPyP})]_2$ (**23**), were also obtained by us from the corresponding ruthenium precursors. According to solution NMR and solid-state X-ray data, in both cases, the staggered conformers form exclusively.[25]

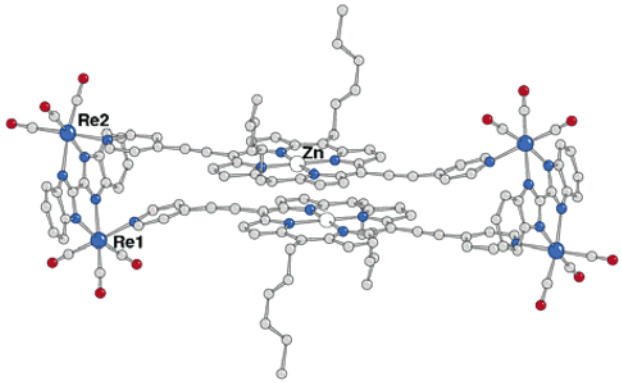

FIGURE 9. X-ray molecular structure of the cation of **19**. Adapted from ref 24.

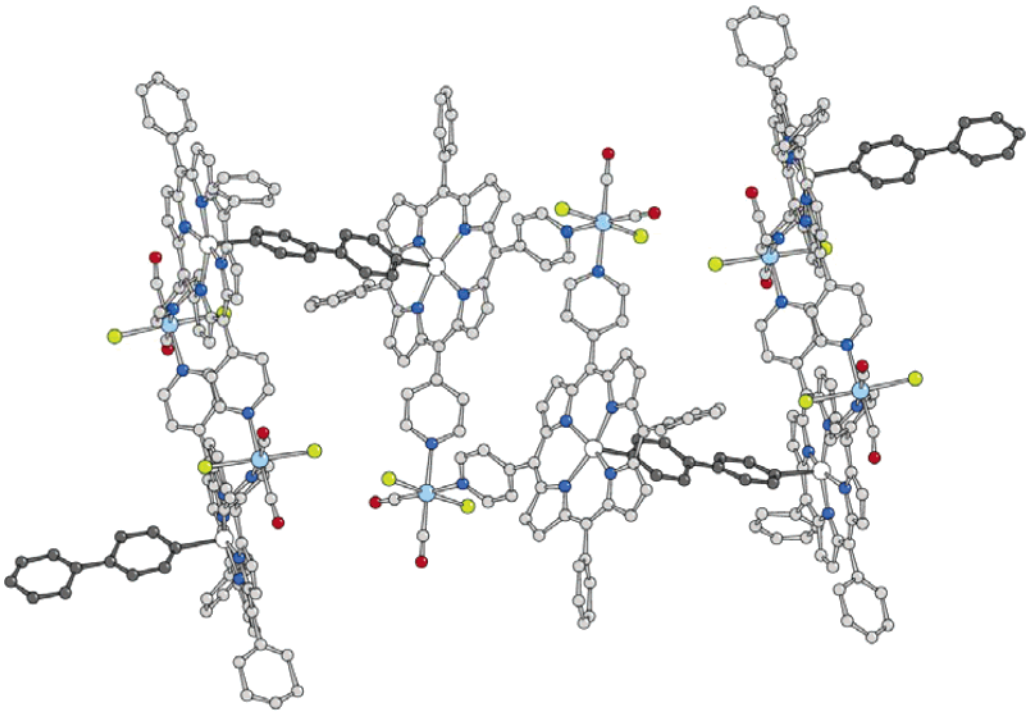

FIGURE 10. Repeating unit in the [(**15Zn**)(μ-4,4′-bipy)]$_n$ polymer. Adapted from ref 21.

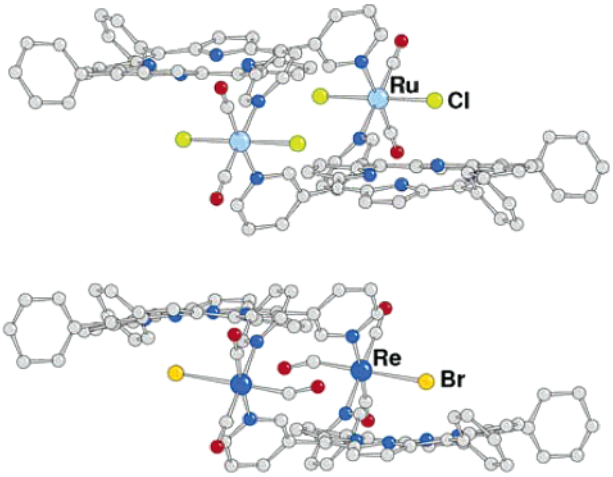

FIGURE 11. X-ray molecular structures of **21** (top, adapted from ref 22) and **24** (bottom, isomer at a higher occupancy of 60%).

A rhenium-mediated porphyrin metallacycle, [ReBr(CO)$_3$(μ-3′-*cis*-DPyP)]$_2$ (**24**), structurally very similar to **21**, was obtained by us upon the reaction of the Re^{I} precursor ReBr(CO)$_5$ with an equimolar amount of 3′-*cis*-DPyP (Figure 11).[26] In the X-ray molecular structure of **24**, the Br ligands were found disordered over the trans-located CO ligands.

Structures **21**, **21Zn**, and **24** exhibit ideal C_{2h} symmetries, with the 2-fold axis passing through the metals. The Ru ions are separated by 14.16 Å in **21**, while the intermetallic distance in the Re derivative **24** is slightly longer (14.31 Å). Correspondingly, the interplanar distance between the two porphyrins is ca. 4.2 Å in the Ru metallacycles and slightly larger, 4.9 Å, in **24**. These differences are mainly dictated by the larger radius of the Re atom. The porphyrins (which are rather distorted, with displacement of atoms up to 0.5 Å from the best fit plane) are bowed inward in **21**, while they are considerably bowed outward in **24** (Figure 11).

Therefore, we demonstrated that the simple change of position of the peripheral pyridyl nitrogen atoms from 4′ to 3′ in the *cis* bifunctional donor ligand (4′-*cis*-DPyP versus 3′-*cis*-DPyP) induces, after coordination to the same *cis* bifunctional metal fragment [either *trans*,*cis*-RuCl$_2$(CO)$_2$ or *fac*-ReBr(CO)$_3$], dramatic structural differences in the metallacycles: from flat 2D to staggered 3D geometries with a rigid spatial arrangement of the two chromophores.

There is only one other example of a multiporphyrin discrete assembly obtained by coordination of 3′-PyPs to external metal centers. Fujita and co-workers reported the X-ray structure of a charged tridimensional prism, [{Pd(en)}$_6$(μ-Zn·3′-TPyP)$_3$](NO$_3$)$_{12}$ (**25**, en = ethylenediamine), obtained quantitatively by the reaction of the tetratopic 3′-tetrapyridyl porphyrin (3′-TPyP) with two equivalents of the *cis* bifunctional metal precursor [Pd(en)(ONO$_2$)] (Figure 12).[27] In aqueous media, the hydrophobic hollow cavity of the prism can accommodate neutral organic molecules, such as pyrene and perylene. The compound has a pseudo-3-fold symmetry (D_{3h}), with Pd···Pd distances in a range from 8.87 to 9.66 Å. It is interesting to observe that all pyridyl rings in **25** have a *syn* orientation, with the connecting Pd fragments above adjacent porphyrins (*up*−*up* conformation).

6. Conclusions

Molecular boxes **17** and **18** are particularly stimulating for further investigation, because the two cofacial porphyrins might induce the inclusion of guest molecules of appropriate shape and size through π−π interactions or axial coordination, if suitable metal centers are inserted. We

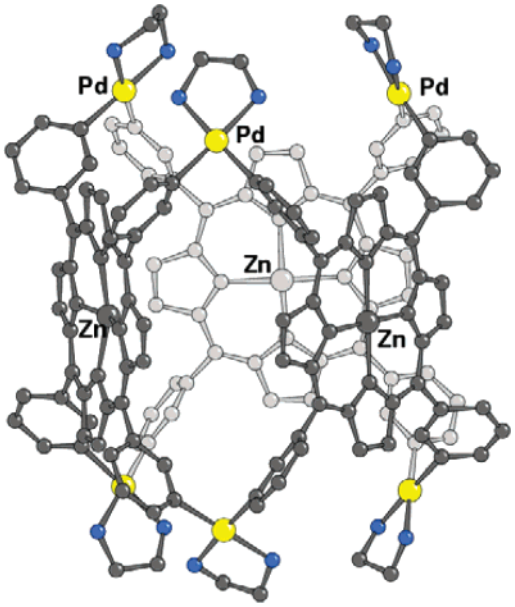

FIGURE 12. X-ray molecular structure of the cation of **25** (Zn ions are axially coordinated by water molecules; not shown for clarity). Adapted from ref 27.

demonstrated that in the molecular box efficient energy transfer occurs from the metallacycles to the bridging porphyrins upon photoexcitation;[5,28] therefore, interesting guests could be molecules to be used as energy or electron acceptors (e.g., aromatic hydrocarbons, aromatic bisimides, and fullerenes). The flexibility of our synthetic approach allows us to change the nature of both modules, the metallacycles and the bridging ligands, at will. Interestingly, when the geometry of the metallacycles is changed (*vide infra*), the distance between the cofacial bridging porphyrins can also be varied.

In particular, we are now interested in exploiting our synthetic approach for the preparation of new *multichromophore* sandwich assemblies using bispyridyl perylene−bisimide dyes (PBIs)[29] as linear bridging ligands between the two porphyrin metallacycles. Indeed, multichromophore assemblies of nanoscopic dimensions that incorporate different light-absorbing units, such as porphyrins and PBIs, offer the greatest chances for light-induced applications.[30] Recently, we prepared the model system [{Ru(TPP)(CO)}$_2$(μ-PBI)], in which two ruthenium−tetraphenyl carbonyl porphyrins are axially bound to a central PBI chromophore, that has an interesting wavelength-dependent photophysical behavior.[31]

In the perspective of metal-mediated assembly of a higher order, the zincated derivatives of the slipped-cofacial porphyrin metallacycles **21**−**24**, obtained by a remarkably simple synthetic procedure, are new additions in the toolbox of building blocks for hierarchical constructions; if **15Zn** is a flat panel with two axial junctions, **21Zn** is the corresponding staggered module. For example, **21Zn** or **24Zn** might be used for the construction of sandwich assemblies similar to **16**−**18** by the reaction with an equimolar amount of a linear ditopic ligand. Interestingly, the distance between the porphyrin centroids is remarkably shorter in the staggered (range of 9.6−10.4 Å) compared to the flat metallacycles (14.0 Å). Thus, multiporphyrin molecular boxes assembled with staggered metallacycles are expected to bring the two bridging porphyrins much closer to each other compared to the "flat" adducts, with an additional vertical offset ranging from 4.2 Å (Ru) to 4.9 Å (Re), corresponding to the height of the step.

We have contributed to the limited database of metal-mediated multiporphyrin assemblies with a remarkable number of X-ray structures, and we found several examples of unexpected geometries and/or distortions. Thus, while thinking of the porphyrins and metal fragments as rigid units is an acceptable approximation for the design of new systems, it may be misleading in the interpretation of spectral data in the absence of X-ray structural determinations.[32] Both the tetrapyrrole macrocycles *and* the metal junctions tolerate significant distorsions imposed by intramolecular stacking interactions, crystal packing, metalation, axial coordination, and steric effects of the ancillary ligands, even when they form small metallacycles. In addition, unless the metal−N(py) and *meso* C−C bonds are all aligned (such as in the adducts of 4′-*trans*-DPyP), rotation about these single bonds adds further degrees of freedom that, in the absence of constraints, may lead to unpredictable geometries. Examples are the pseudo-helicate [**10Zn**]$_2$ and the slipped-cofacial metallacycles **21**−**24**.

Part of this work was supported by the donors of the Petroleum Research Fund, administered by the ACS (Grant ACS PRF 38892-AC3).

References

(1) (a) Vasil'ev, S.; Orth, P.; Zouni, A.; Owens, T. G.; Bruce, D. Excited-state dynamics in photosystem II: Insights from the X-ray crystal structure. *Proc. Natl. Acad. Sci. U.S.A.* **2001**, *98*, 8602−8607. (b) Law, C. J.; Roszak, A. W.; Southall, J.; Gardiner, A. T.; Isaacs, N. W.; Cogdell, R. J. The structure and function of bacterial light-harvesting complex. *Mol. Membr. Biol.* **2004**, *21*, 183−191. (c) Grotjohann, I.; Gromme, P. Structure of cyanobacterial photosystem I. *Photosynth. Res.* **2005**, *85*, 51−72.

(2) Gust, D.; Moore, T. A.; Moore, A. L. Mimicking photosynthetic solar energy transduction. *Acc. Chem. Res.* **2001**, *34*, 40−48.

(3) (a) Choi, M.-S.; Yamazaki, T.; Yamazaki, I.; Aida, T. Bioinspired molecular design of light-harvesting multiporphyrin arrays. *Angew. Chem., Int. Ed.* **2004**, *43*, 150−158. (b) Aratani, N.; Osuka, A.; Cho, H. S.; Kim, D. Photochemistry of covalently-linked multiporphyrin systems. *J. Photochem. Photobiol., C* **2002**, *3*, 25−52.

(4) (a) Baldini, L.; Hunter, C. A. Self-assembly of porphyrin arrays. *Adv. Inorg. Chem.* **2002**, *53*, 213−259. (b) Satake, A.; Kobuke, Y. Dynamic supramolecular porphyrin systems. *Tetrahedron* **2005**, *61*, 13−14. (c) Chambron, J.-C.; Heitz, V.; Sauvage, J.-P. Noncovalent multiporphyrin assemblies. In *The Porphyrin Handbook*; Kadish, K. M., Smith, K. M., Guillard, R., Eds.; Academic Press: San Diego, CA, 2000; Vol. 6, pp 1−42.

(5) (a) Scandola, F.; Chiorboli, C.; Prodi, A.; Iengo, E.; Alessio, E. Photophysiscal properties of metal-mediated assemblies of porphyrins. *Coord. Chem. Rev.* **2006**, *250*, 1471−1496. (b) Iengo, E.; Scandola, F.; Alessio, E. Metal-mediated multi-porphyrin discrete assemblies and their photoinduced properties. *Struct. Bonding* **2006**, *121*, 105−144.

(6) (a) Sanders, J. K. M.; Bampos, N.; Clyde-Watson, Z.; Darling, S. L.; Hawley, J. C.; Kim, H.-J.; Mak, C. C.; Webb, S. J. Axial coordination chemistry of metalloporphyrins. In *The Porphyrin Handbook*; Kadish, K. M., Smith, K. M., Guillard, R., Eds.; Academic Press: San Diego, CA, 2000; Vol. 3, pp 1−48. (b) Bouamaied, I.; Coskun, T.; Stulz, E. Axial coordination to metalloporphyrins leading to multinuclear assemblies. *Struct. Bonding* **2006**, *121*, 1−48.

(7) Abbreviations: 4′-MPyP, 5-(4′-pyridyl)-10,15,20-triphenylporphyrin; 4′-*cis*-DPyP, 5,10-bis(4′-pyridyl)-15,20-diphenylporphyrin; 4′-*trans*-DPyP, 5,15-bis(4′-pyridyl)-10,20-diphenylporphyrin; 4′-*trans*-DPyP-npm, 5,15-bis(4′-pyridyl)-2,8,12,18-tetranormalpropyl-3,7,13,17-tetramethylporphyrin; 4′-TPyP, 5,10,15,20-tetra(4′-pyridyl)-porphyrin.

(8) Alessio, E. Synthesis and reactivity of Ru-, Os-, Rh-, and Ir-halide−sulfoxide complexes. *Chem. Rev.* **2004**, *104*, 4203−4242.

(9) A mixed-ligand dmso/CO precursor, *trans*,*trans*,*trans*-[$RuCl_2$-(dmso-S)$_2$(dmso-O)(CO)], that yields the *trans*,*cis*-$RuCl_2$(dmso-S)-(CO) fragment is also available.

(10) Alessio, E.; Macchi, M.; Heat, S. L.; Marzilli, L. G. Ordered supramolecular porphyrin arrays from a building block approach utilizing pyridylporphyrins and peripheral ruthenium complexes and identification of a new type of mixed-metal building block. *Inorg. Chem.* **1997**, *56*, 5614−5623.

(11) Gianferrara, T.; Serli, B.; Zangrando, E.; Iengo, E.; Alessio, E. Pyridylporphyrins peripherally coordinated to ruthenium-nitrosyls, including the water-soluble Na_4[Zn·4′-TPyP{$RuCl_4$(NO)}$_4$]: Synthesis and structural characterization. *New J. Chem.* **2005**, *29*, 895−903.

(12) Yuan, H.; Thomas, L.; Woo, L. K. Synthesis and characterization of mono-, bis-, and tetrakis-pyridyltriarylporphyrin Pd(II) and Pt-(II) supramolecular assemblies. Molecular structure of a Pd-linked bisporphyrin complex. *Inorg. Chem.* **1996**, *35*, 2808−2817.

(13) Iengo, E.; Zangrando, E.; Alessio, E.; Chambron, J.-C.; Héitz, V.; Flamigni, L.; Sauvage, J.-P. A functionalized noncovalent macrocyclic multiporphyrin assembly from a dizinc(II) bis-porphyrin receptor and a free-base dipyridylporphyrin. *Chem.—Eur. J.* **2003**, *9*, 5879−5887.

(14) Pascard, C.; Guilhem, J.; Chardon-Noblat, S.; Sauvage, J.-P. Molecular structure of an oblique bis-zinc porphyrin 1,10-phenanthroline. Model of a fragment of the photosynthetic reaction centre. *New J. Chem.* **1993**, 331−335.

(15) For the X-ray structure of a *trans* platinum organometallic bisporphyrin complex, see Chen, Y.-J.; Chen, S.-S.; Lo, S.-S.; Huang, T.-H.; Wu, C.-C.; Lee, G.-H.; Peng, S.-M.; Yeh, C.-Y. Porphyrin dimers bridged by a platinum−diacetylide unit. *Chem. Commun.* **2006**, 1015−1017.

(16) (a) Sun, D.; Tham, F. S.; Reed, C. A.; Chaker, L.; Burgess, M.; Boyd, P. D. Porphyrin−fullerene host−guest chemistry. *J. Am. Chem. Soc.* **2000**, *122*, 10704−10705. (b) Sun, D.; Tham, F. S.; Reed, C. A.; Chaker, L.; Boyd, P. D. Supramolecular fullerene−porphyrin chemistry. Fullerene complexation by metalated "jaws porphyrin" hosts. *J. Am. Chem. Soc.* **2002**, *124*, 6604−6612.

(17) Iengo, E.; Milani, B.; Zangrando, E.; Geremia, S.; Alessio, E. Novel ruthenium building blocks for the efficient modular construction of heterobimetallic molecular squares of porphyrins. *Angew. Chem., Int. Ed.* **2000**, *39*, 1096−1099.

(18) Metalation of **10** was not performed because **10Zn** is expected to give auto-aggregation processes in solution, because of interactions between zinc and the oxygen atom of dmso-S.

(19) Iengo, E.; Zangrando, E.; Geremia, S; Graff, R.; Kieffer, B; Alessio, E. Two-point self-coordination of a dizinc(II) bispyridylporphyrin ruthenium complex leading selectively to a discrete molecular assembly: Solution and solid-state characterization. *Chem.—Eur. J.* **2002**, *8*, 4670−4674.

(20) Schmitz, M.; Leininger, S.; Fan, J.; Arif, A. M.; Stang, P. J. Preparation and solid-state properties of self-assembled dinuclear platinum(II) and palladium(II) rhomboids from carbon and silicon tectons. *Organometallics* **1999**, *18*, 4817−4824.

(21) Iengo, E.; Zangrando, E.; Minatel, R.; Alessio, E. Metallacycles of porphyrins as building blocks in the construction of higher order assemblies through axial coordination of bridging ligands: Solution- and solid-state characterization of molecular sandwiches and molecular wires. *J. Am. Chem. Soc.* **2002**, *124*, 1003−1013.

(22) Iengo, E.; Zangrando, E.; Bellini, M.; Alessio, E; Prodi, A.; Chiorboli, C.; Scandola, F. Pyridylporphyrin metallacycles with a slipped cofacial geometry: Spectroscopic, X-ray, and photophysical characterization. *Inorg. Chem.* **2005**, *44*, 9752−9762.

(23) (a) Splan, K. E.; Keefe, M. H.; Massari, A. M.; Walters, K. A.; Hupp, J. T. Synthesis, characterization, and preliminary intramolecular energy transfer studies of rigid, emissive, rhenium-linked porphyrin dimers. *Inorg. Chem.* **2002**, *41*, 619−621. (b) Splan, K. E.; Stern, C .L.; Hupp, J. T. Two coordinatively linked supramolecular assemblies constructed from highly electron deficient porphyrins. *Inorg. Chim. Acta* **2004**, *357*, 4005−4014.

(24) Benkstein, K. D.; Stern, C. L.; Splan, K. E.; Johnson, R. C.; Walters, K. A.; Vanhelmont, F. W. M.; Hupp, J. T. Collapsed molecular rectangles based on rhenium(I) coordination of ethynylpyridyl porphyrins—Synthesis, structure, and bending-induced charge-transfer behavior. *Eur. J. Inorg. Chem.* **2002**, 2818−2822.

(25) Although the structural analysis confirms the geometry for **23**, the accuracy of the geometrical data, heavily affected by the dmso/CO disorder and the crystal quality, is low.

(26) Iengo, E.; Zangrando, E.; Alessio, E. Unpublished results. CCDC reference number 604205.

(27) Fujita, N.; Birhadha, K.; Fujita, M.; Sakamoto, S.; Yamaguchi, K. A porphyrin prism: Structural switching triggered by guest inclusion. *Angew. Chem., Int. Ed.* **2001**, *40*, 1718−1721.

(28) Prodi, A.; Chiorboli, C.; Scandola, F.; Iengo, E.; Alessio, E. Electronic energy transfer in a multiporphyrin-based molecular box. *ChemPhysChem* **2006**, *7*, 1514−1519.

(29) Würthner, F. Perylene bisimide dyes as versatile building blocks for functional supramolecular architectures. *Chem. Commun.* **2004**, 1564−1579.

(30) As expected for truly supramolecular species, the absorption spectra of all of the assemblies described here are always a good superposition of those of the molecular components (see ref 5).

(31) Prodi, A.; Chiorboli, C.; Scandola, F.; Iengo, E.; Alessio, E.; Dobrawa, R.; Würthner, F. Wavelength-dependent electron and energy transfer pathways in a side-to-face ruthenium porphyrin/perylene bisimide assembly. *J. Am. Chem. Soc.* **2005**, *127*, 1454−1462.

(32) Senge, M. O. Exercises in molecular gymnastic-bending, stretching and twisting porphyrins. *Chem. Commun.* **2006**, 243−256.

AR040240+